AGU ADVANCING EARTH AND SPACE SCIENCE

JGR Oceans

RESEARCH ARTICLE
10.1029/2020JC016301

Key Points:
- We present hydrographic observations from a subglacial discharge plume pool and ice mélange adjacent to a Greenland tidewater glacier
- The glacial ice melt fraction in the plume pool is estimated at 1–2% of the total freshwater fraction, increasing to 12% within 2 km
- The interpretation of glacier-derived meltwater stratification depends highly on the types of freshwater sources

Supporting Information:
- Supporting Information S1

Correspondence to:
J. Mortensen,
jomo@natur.gl

Citation:
Mortensen, J., Rysgaard, S., Bendtsen, J., Lennert, K., Kanzow, T., Lund, H., & Meire, L. (2020). Subglacial discharge and its down-fjord transformation in West Greenland fjords with an ice mélange. *Journal of Geophysical Research: Oceans*, *125*, e2020JC016301. https://doi.org/10.1029/2020JC016301

Received 8 APR 2020
Accepted 12 AUG 2020
Accepted article online 27 AUG 2020

Subglacial Discharge and Its Down-Fjord Transformation in West Greenland Fjords With an Ice Mélange

John Mortensen[1], Søren Rysgaard[1,2,3], Jørgen Bendtsen[4], Kunuk Lennert[5], Torsten Kanzow[6,7], Henrik Lund[8], and Lorenz Meire[1,9]

[1]Greenland Climate Research Centre, Greenland Institute of Natural Resources, Nuuk, Greenland, [2]Arctic Research Centre, Department of Bioscience, Aarhus University, Aarhus, Denmark, [3]Centre for Earth Observation Science, CHR Faculty of Environment Earth and Resources, University of Manitoba, Winnipeg, Manitoba, Canada, [4]Norwegian Institute for Water Research, Niva Denmark, Copenhagen, Denmark, [5]The Arctic University of Norway, University of Tromsø, Tromsø, Norway, [6]Alfred-Wegener-Institute, Helmholtz Centre for Polar and Marine Research, Bremerhaven, Germany, [7]Bremen University, Bremen, Germany, [8]Greenland Institute of Natural Resources, Nuuk, Greenland, [9]Department of Estuarine and Delta Systems, Royal Netherlands Institute for Sea Research and Utrecht University, Yerseke, The Netherlands

Abstract Buoyant freshwater released at depth from under Greenland's marine-terminating glaciers gives rise to vigorous buoyant discharge plumes adjacent to the termini. The water mass found down fjord formed by mixing of buoyant subglacial freshwater and ambient fjord water and subsequent modification by glacial ice melt in the ice mélange is referred to as subglacial water. It substantially affects both the physical and chemical properties of the fjords' marine environment. Despite the importance of this freshwater source, many uncertainties remain regarding its transformation and detection. Here we present observations close to a marine-terminating glacier in a fjord with substantial ice mélange and follow the down-fjord changes of the subglacial discharge plume. Heat brought to the surface by entrainment of warm ambient fjord water into the rising plume causes intense melting of the ice mélange close to the plume pool. This results in an increase of glacial ice melt fraction to total glacial meltwater from 1–2% in the plume pool to ~18% eleven kilometers down-fjord, with the largest increase being observed within the first few kilometers. Down-fjord of the ice mélange two temperature minima bound the layer containing subglacial water. The upper bound is linked to the adjacent ice mélange and down-fjord runoff sources, whereas the lower bound is linked to the stratification of the ambient water. We show that similar bounds can be observed in other marine-terminating glacier fjords along West Greenland that contain an ice mélange, suggesting that similar processes work in other fjords.

1. Introduction

The changing freshwater discharge from the Greenland ice sheet has motivated recent studies to assess the freshwater transport from the Greenland ice sheet to the open ocean (e.g., Dukhovskoy et al., 2019; Yang et al., 2016). In fjords, freshwater has been linked to changes in physical properties (water masses) and circulation (e.g., Mortensen et al., 2011; Straneo et al., 2011) with major consequences for carbon chemistry (Rysgaard et al., 2012; Seifert et al., 2019), nutrient dynamics, and local and regional ecosystems (Cape et al., 2019; Hopwood et al., 2018; Meire et al., 2017). On broader scales, freshwater from the Greenland ice sheet has been linked to global sea level rise (Hanna et al., 2013; Rietbroek et al., 2016), changes in the convection driving the North Atlantic thermohaline circulation (Fichefet et al., 2003; Rahmstorf, 1995; Stouffer et al., 2006; Thornalley et al., 2018; Wu et al., 2004), and changes in primary production (Kwiatkowski et al., 2019).

During summer, the largest freshwater sources to fjords in Greenland are as follows: glacier meltwater formed on the glacier surface and discharged at the grounding line of marine-terminating and land-terminating glaciers, and glacial ice discharged in association with calving. For marine-terminating glaciers, the subglacial meltwater discharge happens well below the ocean surface. The water mass is called *subglacial freshwater* while the discharge is referred to as *subglacial discharge*. In connection with land-terminating glaciers the discharge takes place to the surface layer. The water mass is called *freshwater* and discharge is referred to as *runoff*. In fjords where freshwater sources comprise subglacial and glacial ice discharge, the water mass formed down-fjord by subglacial discharge has been referred to as *glacially*

modified water (e.g., Beaird et al., 2018; Carroll et al., 2015; Straneo et al., 2011). In fjords where freshwater sources comprise subglacial discharge, runoff, and glacial ice discharge, the water mass formed down-fjord by subglacial discharge has been referred to as *subglacial water* (Mortensen et al., 2011, 2013). This terminology distinguishes between different pathways—shallow runoff and deep subglacial discharge—taken by meltwater from the glacier surface. We thereby ensure that water masses formed by freshwater taking different pathways do not end up being interpreted as the same water mass, that is, glacially modified water.

Marine-terminating glaciers drain 88% of the ice sheet area in Greenland (Rignot & Mouginot, 2012), the remainder being land-terminating glaciers that ultimately drain to the ocean through rivers. The fjords' stratification and dynamics associated with the discharge from these glaciers have been studied using both observations (Bendtsen, Mortensen, Lennert, et al., 2015; Chauché et al., 2014; Jackson et al., 2017; Mankoff et al., 2016; Mortensen et al., 2013; Motyka et al., 2003; Stevens et al., 2016) and models (Bendtsen, Mortensen, & Rysgaard, 2015; Carroll et al., 2015; Jenkins, 2011; Slater et al., 2015). However, significant gaps remain in our knowledge of the pathways and transformation of subglacial freshwater in fjord systems with marine-terminating glaciers.

Subglacial discharge combined with entrainment of warm ambient subsurface water as the buoyant plume rises can lead to a "plume pool," defined here as the ice-free opening in the ice mélange close to the fronts of marine-terminating glaciers. For logistical reasons, few *in situ* measurements have been obtained in plume pools. So far, hydrographic observations have only been reported from a few (~5) plume pools next to tidewater outlet glaciers in Greenland (Bendtsen, Mortensen, Lennert, et al., 2015; Chauché et al., 2014; Jackson et al., 2017; Mankoff et al., 2016). These studies all showed the same general picture of the plume pool as a water mass that mainly originates from mixing of subglacial freshwater and warmer ambient fjord water at depth with limited influence of submarine melting of the glacier front.

Glacial ice discharge to many Greenland fjord systems with larger marine-terminating glaciers is associated with an adjacent ice mélange, a mix of calved glacier ice and sea ice found close to their terminus, for example, in Ilulissat Icefjord (Amundson et al., 2010), Sermilik Fjord (Cape et al., 2019), and Godthåbsfjord (Motyka et al., 2017). The ice mélange forms when the addition of calved glacier ice is faster than the melt and transports away from the terminus and becomes so dense that it is extremely difficult to navigate by any kind of surface vessel. The mélange alters the fjord dynamics and thermodynamics and affects water mass properties down-fjord. Given the potential significance of interactions between the mélange and the fjord water, we need an improved understanding of these systems. However, of the four studies with data from plume pools mentioned above, only the study by Bendtsen, Mortensen, Lennert, et al. (2015) was conducted in a fjord with an ice mélange.

In this paper we present new hydrographic observations from a plume pool and ice mélange adjacent to the marine-terminating glacier Kangiata Nunaata Sermia (KNS) in Godthåbsfjord (Nuup Kangerlua), in Southwest Greenland (Figure 1). Our data include hydrographic profiles within the plume pool, the ice mélange and further down-fjord. Our analysis, based on interpretation of water masses, mixing between them, and interactions with the ice front and an ice mélange, leads to new insight on melt rates and stratification in fjords with an extensive ice mélange and two different freshwater sources (i.e., runoff and subglacial freshwater discharge).

2. Study Area and Methodology

2.1. Settings

Godthåbsfjord (Nuup Kangerlua) is located in Southwest Greenland and is one of the largest fjord systems in Greenland in terms of surface area. The main fjord branch is 190 km long and the fjord system covers an area of 2,013 km^2 (Figure 1). Godthåbsfjord is in contact with three marine-terminating tidewater outlet glaciers which supply subglacial freshwater at depth to the fjord. The grounding line depths of the three tidewater outlet glaciers have been estimated at <250, <140, and <160 m for Kangiata Nunaata Sermia, Akullersuup Sermia, and Narsap Sermia, respectively. Additionally, three land-terminating glaciers, Qamanaarsuup Sermia, Kangilinnguata Sermia, and Saqqap Sermersua, supply runoff from the Greenland ice sheet to the fjord's surface layer.

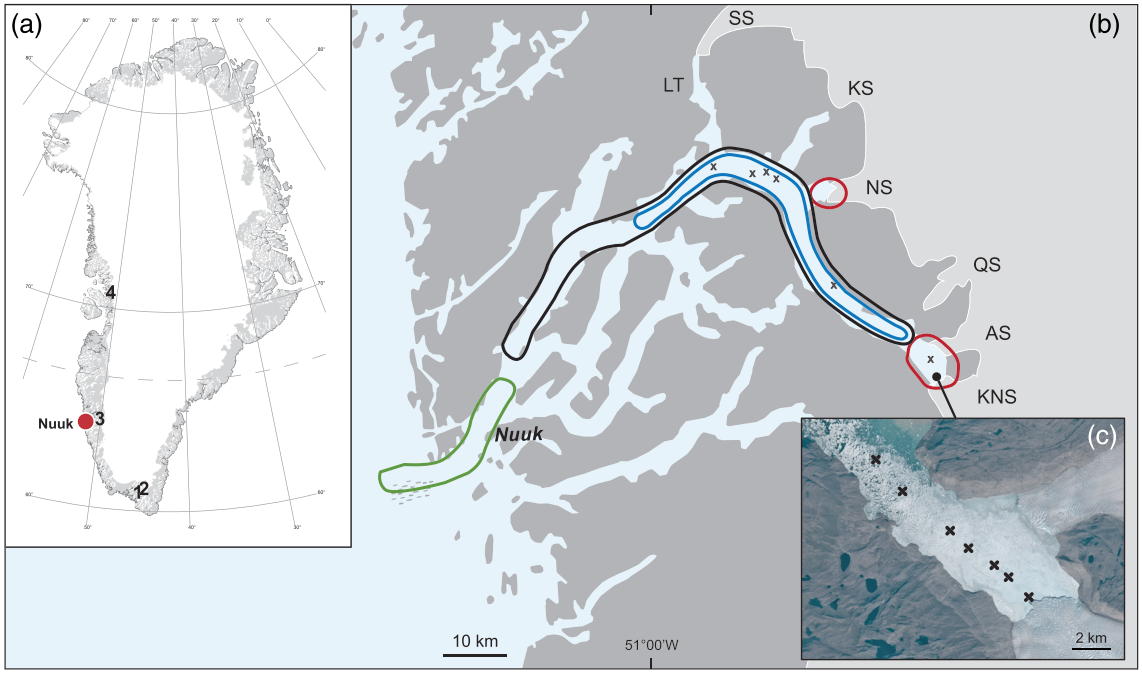

Figure 1. (a) Map of Greenland indicating the positions of the four fjords covered by the present study: Bredefjord (1), Skovfjord (2), Godthåbsfjord (3), and Store Fjord (4); (b) map of the Godthåbsfjord system and the adjacent continental shelf and slope, showing hydrographic stations and XCTDs as crosses. The outer sill region, main fjord branch, inner fjord, and two ice mélanges are indicated as green, black, blue, and red closed areas, respectively. Marine-terminating glaciers: KNS, Kangiata Nunaata Sermia; AS, Akullersuup Sermia; NS, Narsap Sermia. Land-terminating glaciers: QS, Qamanaarsuup Sermia; KS, Kangilinnguata Sermia; SS, Saqqap Sermersua; and a lake: LT, Lake Tasersuaq; (c) distribution of XCTD stations marked on pan-sharpened Landsat 8 image from 2 August 2015, rendered with Google Earth Engine.

The summer circulation system in Godthåbsfjord is characterized by three circulation modes with different driving forces. Figure 2 summarizes our present knowledge of the summer circulation system and distribution of water masses in Godthåbsfjord. Two of the circulation modes are associated with freshwater discharge during the summer melt season (i.e., runoff and subglacial freshwater discharge indicated in

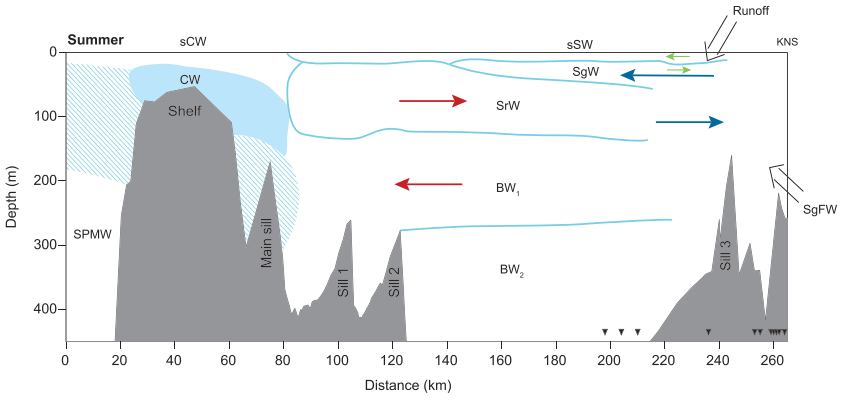

Figure 2. Schematic representation of present knowledge of the circulation system and distribution of water masses in Godthåbsfjord during summer (based on Mortensen et al., 2011, 2013, 2014). CW: Coastal water; sCW: Summer coastal water; SPMW: subpolar mode water; BW_i: basin water types $i = 1–2$; SrW: sill region water; SgW: subglacial water; sSW: summer surface water; SgFW: subglacial freshwater; KNS: Kangiata Nuaata Sermia. Estuarine circulation driven by runoff, small green arrows; subglacial circulation driven by SgFW discharge, large blue arrows; and intermediate baroclinic circulation, red arrows. Inverted triangles in the lower part indicate the location of the occupied XCTDs and down-fjord CTDs. (the basic figure is adapted from Mortensen et al., 2018; Figure 2a, JGR-Oceans).

Figure 3. The plume pool and ice mélange at Kangiata Nunaata Sermia (KNS), Godthåbsfjord, 25 July 2015.

Figure 2): the shallow estuarine circulation driven by runoff and the deeper subglacial circulation driven by subglacial freshwater discharge. The last mode is referred to as the intermediate baroclinic circulation (Figure 2) driven by tidal-induced diapycnal mixing in the outer sill region (Figure 1b). This mixing leads to a horizontal density gradient between the outer sill region and the main fjord and drives the intermediate baroclinic circulation. This circulation mode is present year-round. The stratification of the inner part of Godthåbsfjord (down-fjord sill 3 in Figure 2) and the ice mélange adjacent to KNS is characterized by three layers containing three different water masses: summer surface layer containing summer surface water, subglacial discharge layer containing subglacial water, and ambient water layer containing sill region water. With respect to the abovementioned freshwater sources, the summer surface layer is made up of runoff from land-terminating glaciers, the subglacial discharge layer consists of subglacial freshwater, and the ambient water layer is sill region water, which is a mix of small amounts of both runoff and subglacial freshwater.

The surfacing water mass in a plume pool (see Figure 3) derived from subglacial freshwater before it is modified by marine melt of the ice mélange, is referred to as plume water, as introduced by Chauché et al. (2014). It is highly loaded with sediments and its temperature (T) and salinity (S) properties are found close to the mixing line between subglacial freshwater and ambient water in a T-S plot (section 2.3).

2.2. Methodology

Data were collected using expendable conductivity/temperature/depth profiling probes (XCTD-1 probe, manufactured by Sippican, Inc.) and conductivity, temperature, and depth (CTD) profilers collected by boat.

The XCTDs had a sinking velocity of 3.4 m s^{-1}, a sampling rate of 25 Hz, and temperature and conductivity accuracies of $\pm$0.02°C and $\pm$0.03 mS cm^{-1}, respectively. In the present analysis, we disregard measurements from the first meter. Displayed data were filtered using a 1-s forward-running-mean filter. The XCTD first starts logging when the salinity is above 17, which means we might miss the upper few meters of a potential fresh surface layer in the inner part of Godthåbsfjord.

We deployed two XCTDs by helicopter (Figure 3 and Movie S1 in the supporting information) into a subglacial discharge plume pool less than 20 m from the KNS terminus in Godthåbsfjord on 25 July 2015. Another six XCTDs were deployed through small openings in the ice mélange down-fjord from the terminus along the fjord's center axis within 1.5 to 11 km of the terminus (Figure 1c); a compactly frozen ice mélange

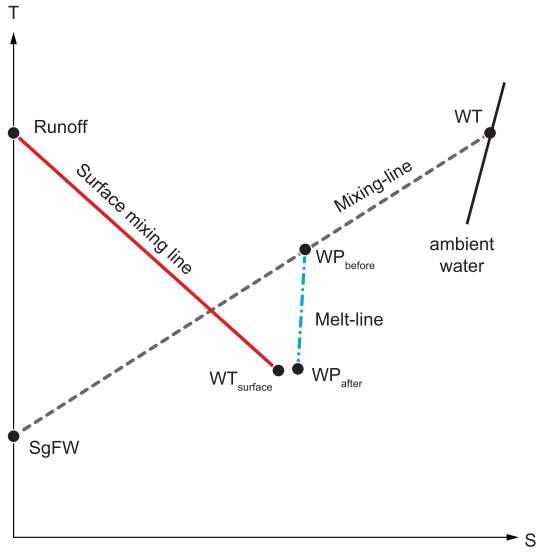

Figure 4. Schematic of the fingerprints of different characteristic freshwater sources in *T-S* space. Mixing of the subsurface source water type (WT) with the discharge of subglacial freshwater (SgFW) leads to mixing products found along the "mixing line." Black solid line = ambient water. Changes of a water parcel (WP) before and after melting of ice. Mixing of the surface water type ($WT_{surface}$) with surface runoff.

prevented sampling closer than 1.5 km from the plume pool. All eight XCTDs were deployed within a period of 34 min.

Additionally, profiles were collected using a CTD profiler (Sea-Bird Electronics SBE19plus SEACAT Profiler). The sensors were calibrated yearly by the manufacturer and uncertainty of salinity was typically within the range 0.005–0.010. All profiles were averaged vertically in 1-m intervals. Four down-fjord CTD profiles were obtained between 28 and 66 km down-fjord in the inner part of Godthåbsfjord between 7 July and 14 August 2015 (Figures 1b and 2). The CTD profiles were usually occupied at the edge of a dense ice field during cruises to the inner part of Godthåbsfjord. The profiles were occupied relatively far from the ice mélange limit. Additionally, CTDs were collected in inner part of four fjords in 2017 and 2018: Bredefjord, Skovfjord, Godthåbsfjord, and Store Fjord (Figure 1a and Table 2).

2.3. Interpretation of Meltwater in *T-S* Space

The three major freshwater sources impacting fjord hydrography and resulting in changes in *T-S* space are as follows: runoff (glacier derived), subglacial freshwater, and submarine melt of glacial ice (below, runoff from land and precipitation-evaporation are assumed negligible during the summer months compared to glacier-derived runoff; Langen et al., 2015). These three major sources all have characteristic fingerprints in *T-S* space allowing them to be identified by their *T-S* characteristics (Figure 4). Mixing between any pair of water types leads to a straight line in *T-S* space.

Mixing of subglacial freshwater (characterized by $T \sim 0°C$ and $S = 0$) with the subsurface source water type (WT) leads to a mixing product found along the "mixing line" in Figure 4. Subglacial freshwater discharge will reveal itself as a halocline (i.e., a salinity gradient) that cannot be explained by the properties of ambient water masses, while thermodynamic changes due to melting of ice produces water mass properties along a "melt line" (Gade, 1979). Figure 4 shows one of many "melt lines" associated with a water parcel before (WP_{before}) and after (WP_{after}) melt. Also shown in Figure 4 is the mixing of the surface water type with runoff; in principle this is a "surface mixing line" in the case of no atmospheric heat exchange with the surface water. The temperature of the runoff depends on the source and will likely be close to the *T-S* properties of subglacial freshwater. The temperature will rise in summer primarily due to solar insolation of the shallow summer surface layer. The presence of a strong shallow surface halocline indicates a significant runoff source in the fjord, and this stratification is not related to the ice mélange.

2.4. Subglacial Freshwater Fraction Model

Below we use the suggested fraction model by Washam et al. (2019) that uses observed potential temperature (Θ_{obs}) and practical salinity (S_{obs}) for calculating the subglacial freshwater fraction (f_{SgFW}) and glacial ice melt fraction (f_i), based on Θ-S properties of subglacial freshwater (Θ_{SwFW}, S_{SgFW}), an artificial submarine glacial melt water (Θ_{SGMW}, S_{SGMW}) and water type (Θ_{WT}, S_{WT}).

$$f_i = 100 \times \frac{(\Theta_{obs} - \Theta_{WT}) - \left((S_{obs} - S_{WT})\left(\Theta_{SgFW} - \Theta_{WT}\right)\right)/\left(S_{SgFW} - S_{WT}\right)}{(\Theta_{SGMW} - \Theta_{WT}) - \left((S_{SGMW} - S_{WT})\left(\Theta_{SgFW} - \Theta_{WT}\right)\right)/\left(S_{SgFW} - S_{WT}\right)} \quad (1)$$

and

$$f_{SgFW} = 100 \times \frac{\left(\Theta_{obs} - \Theta_{WT}\right) - \left((S_{obs} - S_{WT})\left(\Theta_{SGMW} - \Theta_{WT}\right)\right)/(S_{SGMW} - S_{WT})}{\left(\Theta_{SgFW} - \Theta_{WT}\right) - \left(\left(S_{SgFW} - S_{WT}\right)\left(\Theta_{SGMW} - \Theta_{WT}\right)\right)/(S_{SGMW} - S_{WT})} \quad (2)$$

The effective temperature of submarine glacial melt water, which considers the latent heat required to melt ice (Gade, 1979), was calculated following Beaird et al. (2018) as

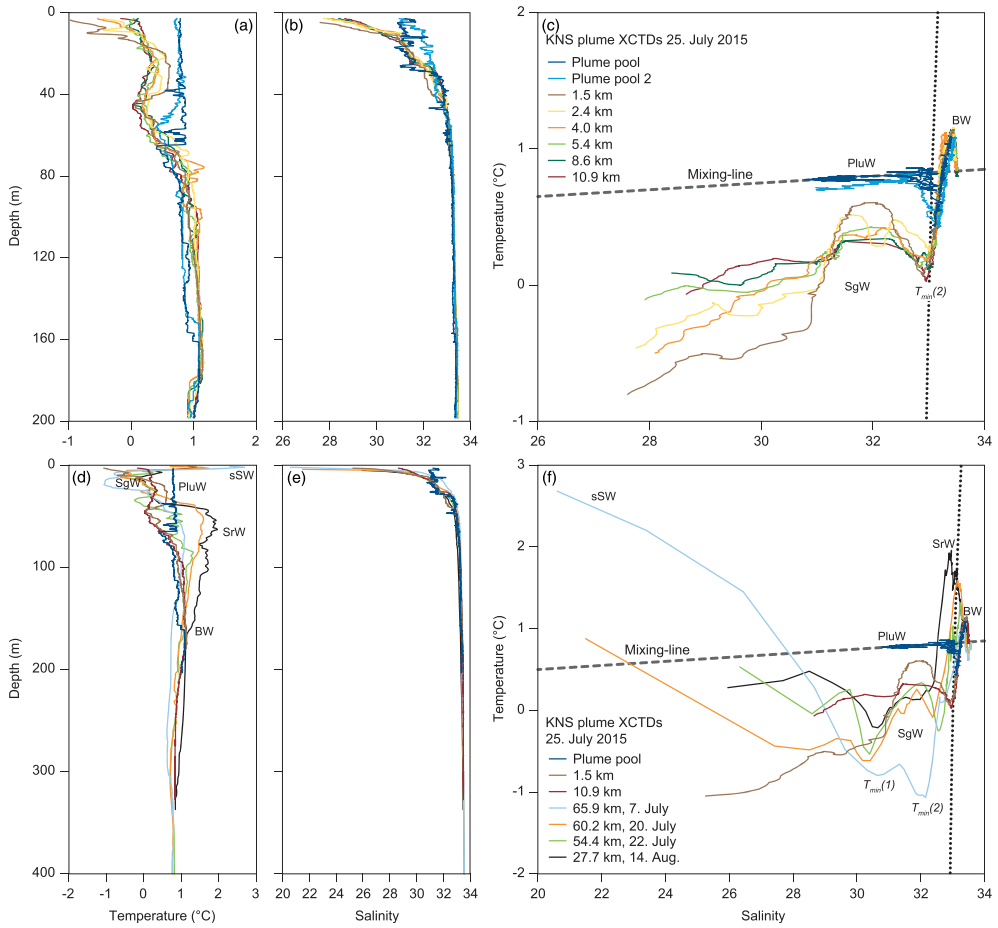

Figure 5. Profiles of (a) temperature (t), (b) salinity (S), and (c) T-S plot for hydrographic stations occupied by XCTDs in and next to the subglacial discharge plume pool of KNS, Godthåbsfjord, 25 July 2015. Down-fjord profiles of (d) temperature (T), (e) salinity (S), and (f) T-S plot for hydrographic station occupied by CTDs in the period 7 July to 14 August 2015. Fjord water masses are indicated in panels (c), (d), and (f): Summer surface water (sSW); plume water (PluW); subglacial water (SgW); sill region water (SrW); basin water (BW). Panels (c) and (f) also show $T_{min}(1)$, $T_{min}(2)$, mixing line (explained in the text), and the 26.5 isopycnal (dotted line). In panel (f) $T_{min}(1)$ and $T_{min}(2)$ are shown only for the 7 July 2015 occupation. Measurements with salinity less than 26 are not shown in (b) and (c); and measurements with salinity less than 20 are not shown in (e) and (f).

$$\Theta_{SGMW} = \Theta_f - \left(L/c_p\right) - \left(c_i/c_p\right)\left(\Theta_f - \Theta_i\right) \tag{3}$$

– where c_i and c_p are the specific heat capacities of ice and seawater, L the latent heat of fusion, temperature of ice (Θ_i), and freezing temperature (Θ_f). The effective temperature of submarine glacial melt water (Θ_{SGMW}) not shown in Figure 4 is found in the range −95.5°C to −86.7°C depending on the choice of temperature of ice and freezing temperature.

3. Results and Discussion

3.1. The Subglacial Discharge Plume and Its Down-Fjord Development

3.1.1. Plume Pool

In the summer of 2015 two XCTDs were deployed in the plume pool, separated by 12 m but both within 20 m of the ice front (terminus). The plume pool is highly dynamic, with vigorous visible turbulence (Movie S1). The two plume pool XCTDs obtained similar T-S profiles that are distinctly warmer close to the surface than the T-S profiles down-fjord (Figures 5a–5c). Temperatures of the subglacial discharge plume increase during the ascent toward the surface by entrainment of ambient heat. The plume pool T-S profiles reveal a 56- to 66-m-thick surface layer (determined by the temperature minimum at the transition to ambient water) of warm

Table 1
Mean Temperature (°C) and Salinity of the Subglacial Discharge Layer Here Defined as the Layer Between 10 and 43.5 m Depth Along the XCTDs Section With Distance (km) From the plume pool observation, 25 July 2015

Distance (x, km)	<T>	<S>	$<f_{SgFW}>$ (%)	$<f_i>$[a] (%)	$<f_i>/(<f_{SgFW}> + <f_i>)$ (%)	$<f_i>_x/<f_i>_{10.9km}$ (%)	$D_{Tmin(2)}$ (m)	Melt (m/day)
0	0.784	31.991	3.81	0.04	1.0	5.8	66	0.09
0.0 (cast 2)	0.770	32.364	2.66	0.06	2.2	8.7	56	
1.46	0.406	31.793	3.98	0.47	11.6	68.1	44	0.17
2.37	0.370	32.008	3.28	0.51	13.5	73.9	47	0.02
4.01	0.302	31.943	3.40	0.59	14.8	85.5	45	0.02
5.39	0.280	31.996	3.22	0.61	15.9	88.4	41	0.008
8.59	0.244	32.000	3.16	0.66	17.3	95.7	45	0.009
10.90	0.213	31.963	3.23	0.69	17.6	100	46	0.008

Note. Also shown are calculated mean layer subglacial freshwater fraction ($<f_{SgFW}>$) and mean layer glacial ice melt fraction ($<f_i>$). Also shown are $<f_i>/(<f_{SgFW}> + <f_i>)$, $<f_i>_x/<f_i>_{10.9km}$ in percent, depth of $T_{min}(2)$, and modeled melt per day of terminus and ice mélange for a subglacial discharge of 100 $m^3 s^{-1}$.
[a]Assuming $T_i = -5$°C and $T_f = -1.5$°C. $(T_{WT},S_{WT}) = (0.85°C,33.27)$, $(T_{SgFW},S_{SgFW}) = (0°C,0)$, and $(T_{SGMW},S_{SGMW}) = (-87.4°C,0)$.

and saline plume water with properties close to the mixing line connecting subglacial freshwater ($T \sim 0$°C; $S = 0$) with ambient fjord water (Figure 5c and 5f). Below ~66 m, the XCTDs leave the plume water and continue to descend into ambient water with T-S profiles matching ambient water registered down-fjord (Figure 5c), that is, the XCTDs are no longer falling in the rising subglacial discharge plume, but just next to it as indicated in Figure 7a (temperature profile associated with Region 1). However, details of the T and S depth profiles (Figure 5a and 5b) show differences. Between 100 and 160 m depth the temperatures are ~0.2°C lower in the two plume pool XCTD profiles compared to the down-fjord XCTD profiles (Figure 5a), whereas the salinity profiles show salinity ~0.1 lower (Figure 5b). The lower temperatures and salinities may be explained by melting of the terminus and may be the origin of the meltwater intrusions recently described by Jackson et al. (2020) or a dynamic process, such as sinking of ambient water from above close to the rising subglacial discharge plume. Some recent model results by, for example, Carroll et al. (2015) and Slater et al. (2017), suggest that plume water sinks back to relatively deep neutral buoyancy levels down-fjord close to the terminus. We here note that sinking of plume water should not be confused with the depth change when the plume water meets the fjord's summer surface layer down-fjord which is discussed below.

3.1.2. Ice Mélange

The T-S profiles of the down-fjord XCTDs (Figure 5a–5c) occupied in the ice mélange are quite similar to each other and reveal a ~44-m-thick surface layer. Recall that the surface layer in fjords may be highly stratified as seen in Figure 5b—unlike surface layers in the open ocean which are generally mixed. The water mass in this layer is referred to as subglacial water and is markedly cooler than the plume water observed in the plume pool (Figures 5a and 5c). Subglacial water forms when plume water is cooled by melting of the ice mélange and has previously been observed down-fjord (Mortensen et al., 2011, 2013, 2018). The layer containing subglacial water is referred to as the *subglacial discharge layer* (Mortensen et al., 2013), where the transition between the subglacial discharge layer and ambient water below is delimited by the temperature minimum $T_{min}(2)$ in Figure 5c. As stated previously, it is important to distinguish between the different freshwater sources (i.e., runoff, subglacial freshwater discharge and glacial ice melt), therefore the terms "subglacial water" and "subglacial discharge layer" are used to point to the origin of the subglacial freshwater discharge source. Salinity variations with depth are pronounced in the subglacial discharge layer

Table 2
Position and Characteristics of Sampled Fjords in West Greenland

Fjord	Date	Latitude (°N)	Longitude (°W)	Distance to terminus (km)	$T_{min}(1)$ - $T_{min}(2)$ (m)	Terminus depth (m)	Sill depth (m)
Bredefjord	2018-07-02	60 56.59	46 16.82	~60	23–66	~50	330[a]
Skovfjord	2018-07-03	61 02.76	45 29.54	~25	15–59	~250	—
Godthåbsfjord	2018-08-09	64 41.64	50 22.23	~19	7–34	~200	~200
Store Fjord	2017-08-17	70 28.64	51 34.83	~39	35–121	~500	~430

[a]Estimated value.

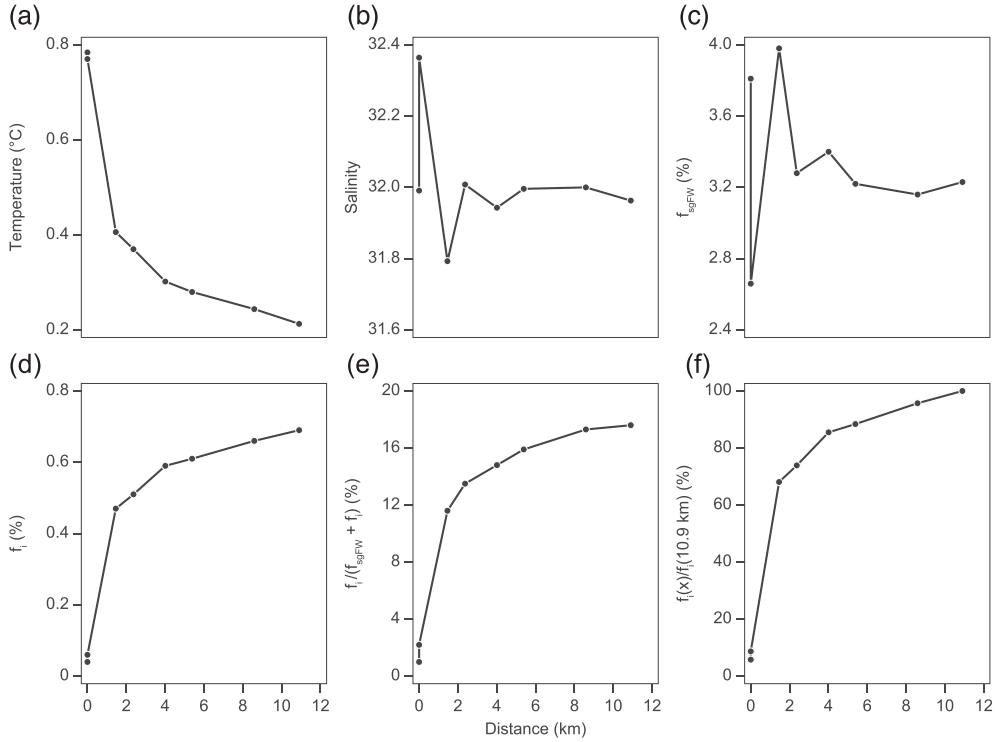

Figure 6. Down-fjord evolution of mean (a) temperature, (b) salinity, (c) subglacial freshwater fraction $\langle f_{SgFW} \rangle$, (d) glacial ice melt fraction $\langle f_i \rangle$, (e) glacial ice melt to total glacial meltwater ratio $\langle f_i \rangle / (\langle f_{SgFW} \rangle + \langle f_i \rangle)$, and (f) glacial ice melt to glacial ice melt 10.9 km from the plume pool ratio $\langle f_i \rangle_x / \langle f_i \rangle_{10.9km}$, in the layer between depths of 10 and 43.5 m along the transect from the plume pool to a point 11 km down-fjord in the ice mélange.

but small in the ambient water layer below 44 m (Figure 5b). Table 1 and Figure 6 show the evolution of mean T (i.e., cooling) and S in the layer at depths between 10 and 43.5 m along the transect from the plume pool to a point 11 km down-fjord in the ice mélange (thus, disregarding the shallow surface layer). Table 1 and Figure 6 also show the calculated fraction of subglacial freshwater ($\langle f_{SgFW} \rangle$) and glacial ice melt ($\langle f_i \rangle$) (Mortensen et al., 2013), the ratio of glacial ice melt to total glacial meltwater $\langle f_i \rangle / (\langle f_{SgFW} \rangle + \langle f_i \rangle)$, and the ratio of glacial ice melt to glacial ice melt 10.9 km from the plume pool $\langle f_i \rangle_x / \langle f_i \rangle_{10.9\text{km}}$. An approximate subglacial freshwater fraction model was used for the calculation developed by Washam et al. (2019) (see above), which introduces an artificial submarine glacial melt water mass (T_{SGMW}, S_{SGMW}).

The observed mean T decreases exponentially with distance from the plume pool due to melt of the ice mélange, whereas mean S is much less affected by the melt process due to the steep melt line associate with melt shown in Figure 4. This is also clear from the fractions calculated in Table 1 and Figure 6. The XCTD data suggest that melting of ice is most intense close to the plume pool and diminishes rapidly with distance down-fjord. Variations in observed mean S highlight temporal variability of the system with respect to water mass distribution, circulation, and subglacial discharge fluxes.

As $\langle f_i \rangle$ and mean T, and $\langle f_{SgFW} \rangle$ and mean S are tightly linked the calculated fractions therefore support the abovementioned mean T and S findings (Figure 6). The fraction of subglacial freshwater remains stable about 3–4% both in the plume pool and down-fjord ice mélange profiles. This suggests that there is not much additional mixing with ambient water down-fjord, which is consistent with the stability of the $T_{\min}(2)$ depth, Table 1. The only cause of variability in T and $\langle f_i \rangle$ is ice mélange melt. The average observed freshwater content in the depth range 1 to 10 m in the plume pool was between 5.6% and 7.1%, corresponding to a mixing ratio between subglacial freshwater and ambient water between 1:13 and 1:16. These values are similar to those reported by Bendtsen, Mortensen, Lennert, et al. (2015)—numbers 7.3% and 1:13, respectively—for the same marine-terminating outlet glacier. In Saqqarliup Fjord in central Greenland, Mankoff et al. (2016) previously reported a 1:10 surface mixing ratio of subglacial freshwater to ambient fjord waters.

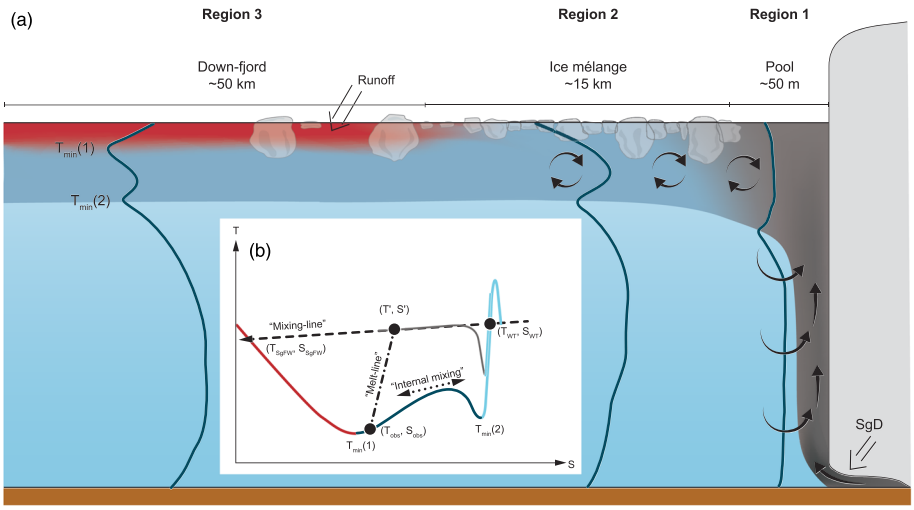

Figure 7. (a) Conceptual figure of the settings within the three regions: Region 1, plume pool; Region 2, ice mélange; Region 3, down-fjord the ice mélange. Plume water (gray-brownish), subglacial water (dark blue), ambient water (light blue), and surface water (red). Characteristic temperature profiles and length scales are shown for the three regions. Subglacial discharge (SgD) and the eventual sinking of ambient water in connection with the rising subglacial discharge plume is indicated. (b) Schematic *T*-*S* representation of the transformation from the plume pool profile to the down-fjord profile with an ice mélange in between and the development of subglacial freshwater by mixing processes and thermodynamic changes associated with melting of an ice mélange. The observed temperature and salinity characteristics (T_{obs}, S_{obs}) in the down-fjord curve are due to mixing of a source water type (T_{WT}, S_{WT}) with subglacial freshwater (T_{SgFW}, S_{SgFW}), which leads to a mixing ratio determined by (T', S') on the "mixing line" in the plume pool curve. Thermodynamic changes due to melting of ice are indicated by the dashed "melt-line." "Internal mixing" is supposed to be responsible for the cooling of the deeper part of the subglacial discharge layer. The layer containing subglacial water in Region 3 is delineated by two minima in the temperature profile, shown as $T_{min}(1)$ and $T_{min}(2)$ in case of Godthåbsfjord.

The ratio of glacial ice melt fraction ($<f_i>$) to total glacial meltwater ($<f_{SgFW}> + <f_i>$) rises from 1–2% in the plume pool to ~18% eleven kilometers down-fjord, with the largest increase being observed within the first kilometers from the tidewater glacier (Table 1). Only 6% of the glacial ice melt fraction can be ascribed to terminus melt during the ascent of the subglacial discharge plume as shown by $<f_i>_{0km}$ related to $<f_i>_{10.90km}$. We note that some of the previously reported numbers from the fjord (Mortensen et al., 2013) were obtained much further down-fjord (>36 km) than the present observations (<11 km) and under different ambient and subglacial discharge conditions. Further, the different rates of vertical cooling of the subglacial discharge layer as functions of depth (Figures 5a and 5c) along the first 11 km down-fjord from the plume pool indicates that glacial ice melt is most pronounced in the upper 20 m of the water column. Freeboard height of the ice mélange was estimated to be around 2 m on the day of the XCTD deployments (Figure 3), suggesting an ice mélange with mean depth of less than 20 m.

Glacial ice discharge by calving from KNS (width: 4,000 m; height: 300 m: glacier speed: 15 m day^{-1}) is about $18{\cdot}10^6$ m^3 day^{-1} (Mortensen et al., 2013). Assuming a subglacial discharge of 100 m^3 s^{-1} and subglacial freshwater and glacial ice melt fractions of 3.81% and 0.69% (Table 1), respectively, this will result in a glacial ice melt of ~$1.6{\cdot}10^6$ m^3 day^{-1} within the first 11 km down-fjord from the terminus (glacial ice melt can be calculated as follows: subglacial discharge * $<f_i>_{10.9km}/<f_{SgFW}>_{0.0km}$). This estimate assumes that the mid-fjord observations are representative of the full width of the fjord. The calculation implies that a 10 times larger subglacial discharge of ~1,000 m^3 s^{-1} would result in a glacial ice melt that would completely melt the glacial ice discharged by calving and thus eliminate the ice mélange in front of the terminus. This is consistent with observations of ice mélange-free conditions in front of the terminus of Narsap Sermia in Godthåbsfjord during the violent drainage of an ice-dammed lake (Kjeldsen et al. (2014) their Video S1). Mankoff et al. (2020) recently estimated the seasonal maximum for total glacial ice derived runoff to the southern glaciers in Godthåbsfjord at ~1,000 m^3 s^{-1}. Further, assuming that the ice mélange is a uniform thick slab of ice and using the fractional increase of $<f_i>_x/<f_i>_{10.9km}$, we have calculated the melt rates

per day of the terminus and of the ice mélange down-fjord segments for a subglacial discharge of 100 $m^3\ s^{-1}$ shown in Table 1 (terminus melt calculated as follows: $1.6{\cdot}10^6\ m^3\ day^{-1}$ * 0.058 / (4,000 m*250 m); first 1.46 km of ice mélange calculated as: $1.6{\cdot}10^6\ m^3\ day^{-1}$ * (0.681–0.058) / (4,000 m * 1,460 m)). The melt rates reveal that terminus melt, and ice mélange melt during the first 1.5 km down-fjord are of the same magnitude (0.09 and 0.17 m day^{-1}, respectively). Although the melt rates are comparable, the melt area of the terminus is much smaller than the ice mélange area which makes a huge difference in volume of glacial ice melt.

3.1.3. Inner Fjord Down-Fjord of the Ice Mélange

CTD profiles obtained in the inner part of the fjord, ~28 to ~66 km from the plume pool at the terminus (Figure 2), and well down-fjord from the outer edge of the ice mélange (Figure 5d–5f), show the subglacial discharge layer positioned between a shallow warm and a fresh summer surface layer (derived from runoff) and the deeper, warmer, and saline ambient water layer. The transition between the summer surface layer and subglacial discharge layer is delimited by the temperature minimum $T_{min}(1)$, previously described by Mortensen et al. (2013), whereas the transition between the subglacial discharge layer and the ambient water layer, characterized by a distinctive thermocline (Figure 5f), is delimited by the temperature minimum $T_{min}(2)$. Down-fjord profiles have previously shown that conditions may change relatively quickly during summer (Mortensen et al., 2014, 2018). If the XCTD section had been occupied a few weeks later, warmer ambient water (observed 27.7 km down-fjord on 14 August; Figure 5d) following the fjord's circulation system described in Figure 2 might have arrived and the plume water temperature near the glacier terminus might have been about ~1°C higher than observed. We expect that a higher ambient water temperature will give rise to higher glacial ice melt fractions.

In other West Greenland fjord systems that do not have an ice mélange, a warmer and fresher surface layer is observed much closer to the plume pool (<1 km) as reported by, for example, Mankoff et al. (2016), Stevens et al. (2016), and Jackson et al. (2017). In Godthåbsfjord we detected the summer surface layer derived from runoff 11–15 km from the plume pool and down-fjord of the ice mélange (Figures 5 and 7a).

The two characteristic temperature minima, $T_{\min}(1)$ and $T_{\min}(2)$, seen in Figure 5d–5f are linked to the layered structure of the water masses in the fjord. Down-fjord profiles support the notion that they can be used to delineate the subglacial discharge layer containing subglacial water down-fjord in Region 3 in Godthåbsfjord, as proposed by Mortensen et al. (2013) (Figure 7a). We assume that the *lower* temperature minimum, $T_{\min}(2)$, arises when the newly formed plume water interacts with the stratified ambient water (characterized by cold and fresh water overlying warm and saline water below) shown schematically in Figure 4. The newly formed plume water found along the mixing line connects with the upper part of the stratified ambient water below, creating $T_{\min}(2)$ (Figure 5c). Therefore, $T_{\min}(2)$ is found below the plume water and further down-fjord below the subglacial discharge layer at the transition to the ambient water (Figure 7b). The *upper* temperature minimum, $T_{\min}(1)$, arises when the relatively heavy subglacial water, which has been cooled by melting of the ice mélange, meets the fjord's warm and fresh summer surface layer derived from runoff down-fjord of the ice mélange (Figures 5f and 7a). Runoff of surface-derived glacier meltwater discharged at the grounding line of land-terminating glaciers in Godthåbsfjord gives rise to summer surface layer properties in the range T ~ 2–4°C and S ~ 5–10 (e.g., Figure 4 in Mortensen et al., 2013; Figure 8 in Kjeldsen et al., 2014).

The transformation of subglacial freshwater to subglacial water in Godthåbsfjord is schematically shown in Figure 7a. Also shown is a schematic presentation of a plume pool (Region 1) and down-fjord (Region 3) profiles in a *T*-*S* diagram (Figure 7b). In summary, the transition of the plume pool *T*-*S* profile to down-fjord *T*-*S* profiles is primarily associated with melt of the ice mélange, internal mixing in the subglacial discharge layer, and the appearance of the down-fjord heated and fresh summer surface layer formed from runoff.

3.2. Subglacial Water in West Greenland Fjords

The two temperature minima in the halocline between the summer surface layer and the ambient water layer below are important features for identifying the subglacial discharge layer boundaries in the inner part of Godthåbsfjord down-fjord from the ice mélange. Profiles in other West Greenland fjords show similar features.

In July/August 2017 and 2018, we sampled four tidewater outlet glacier fjords on the west coast of Greenland: Bredefjord (1: Ikersuaq, ~61°N), Skovfjord (2: Tunulliarfik, ~61°N), Godthåbsfjord (3: ~64°N),

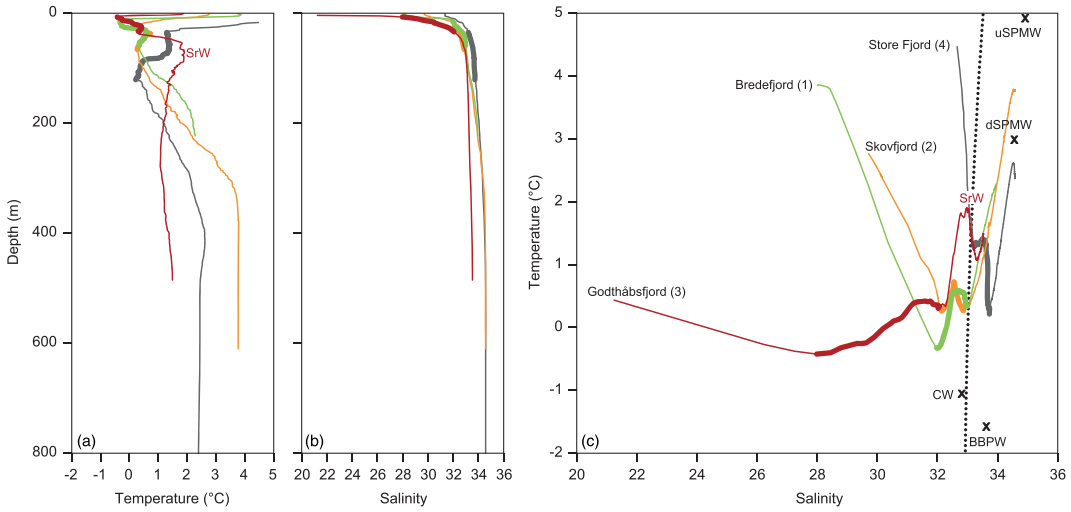

Figure 8. Fjord profiles of (a) temperature (T) (data only shown for $T < 5$°C), (b) salinity (S) (data only shown for $S > 20$), and (c) T-S curves for CTD stations occupied down-fjord of different tidewater outlet glaciers during the subglacial freshwater discharge seasons in 2017 and 2018. Thick line segments show the subglacial discharge layer containing subglacial water. Sill region water (SrW) is indicated in (a) and (c). coastal water masses are indicated in (c): Upper subpolar mode water (uSPMW) and deep subpolar mode water (dSPMW); coastal water (CW); Baffin Bay polar water (BBPW). Also shown in (c) is the 26.5 isopycnal (dotted line). Fjord in (c): Bredefjord (1), Skovfjord (2), Godthåbsfjord (3), and Store Fjord (4).

and Store Fjord (4: ~70°N); Figure 1a and Table 2. All of these fjords were characterized by an ice mélange in front of marine-terminating outlet glaciers. Based on satellite images the outer edge of the ice mélange was estimated for each fjord to be ~8, ~3, ~10, and ~3 km down-fjord for Bredefjord, Skovfjord, Godthåbsfjord, and Store Fjord, respectively. Figure 8 shows down-fjord profiles (Region 3 in Figure 7a) of T, S, and T-S for the different fjords. Despite the large latitudinal gradient and differences in entrance sill depth, glacier characteristics, ice mélange, and down-fjord runoff sources, the fjords show similar hydrographic structure.

In all fjords the halocline located between the summer surface layer and ambient water layer displays the characteristic temperature minima feature associated with subglacial water (Figure 8) as was observed in Godthåbsfjord (section 3.1.3). The depth ranges between the two temperature minima, $T_{\min}(1)$ and $T_{\min}(2)$, are given in Table 2 and indicated by thick line segments in Figure 8. In all fjords, the upper part of the ambient water layer was characterized by a thermocline located just beneath the subglacial discharge layer. In three of the fjords, the transition to ambient water was found close to the mixing line between the two major coastal water masses (Figure 8c) (Rysgaard et al., 2020). In the southern fjords (Bredefjord and Skovfjord), the layer was found close to the mixing line between upper subpolar mode water and coastal water. In the northern fjord (Store Fjord), the layer was found close to the mixing line between deep subpolar mode water and Baffin Bay polar water. In Godthåbsfjord, the associated coastal thermocline layer was found below the layer occupied by sill region water, a locally derived fjord water mass (Figure 8c). The warmest subglacial water, with temperatures above 1°C, was found to the north in Store Fjord which had the smallest extent of ice mélange.

The largest T-S property difference between the four fjords was observed in the summer surface layer linked to the down-fjord runoff sources and their magnitudes. During summer, the runoff to Godthåbsfjord is significant from just one of the three runoff sources: Lake Tasersuaq, which discharges around 1,000 $m^3\ s^{-1}$ or more on daily basis for longer periods, Figure 1b (Kjeldsen et al., 2014).

Despite the differences between the fjord systems, the temperature minima associated with the subglacial discharge layer do seem to be a characteristic feature of the inner parts of marine-terminating glacier fjords with an adjacent ice mélange and down-fjord runoff. In fjords lacking an ice mélange and down-fjord runoff sources conditions are somewhat different. The three near-terminus studies by Chauché et al. (2014), Mankoff et al. (2016), and Jackson et al. (2017) all support the formation of $T_{min}(2)$, whereas only the latter study partly supports the formation $T_{min}(1)$.

4. Summary and Conclusions

Hydrographic measurements in a plume pool at a marine-terminating outlet glacier (KNS) at the head of Godthåbsfjord show that active mixing takes place in the rising subglacial discharge plume; however, most melting of glacial ice takes place in the ice mélange down-fjord from the plume pool. While moving down-fjord, subglacial freshwater undergoes a number of transformations. First, it entrains ambient water during its ascent in the subglacial discharge plume and becomes plume water. Second, it is cooled by the ice mélange and becomes subglacial water. Finally, subglacial water is capped by a shallow warm and fresh summer surface layer as it moves down-fjord from the ice mélange. The shallow summer surface layer is related to advection and (glacier derived) runoff sources down-fjord the ice mélange. The observations reveal that 11 km down-fjord less than 6% of the glacial melt is due to submarine melt of the terminus; the remaining 94% is due to subsequent ice mélange melt. Hydrographic data from XCTD profiles show that melting of the ice mélange is most intense close to the plume pool and diminishes rapidly with distance down-fjord. The subglacial discharge layer is overlain by a shallow, warm, and fresh summer surface layer down-fjord of the ice mélange. This results in a subglacial discharge layer of subglacial water—bound and characterized by two temperature minima—between the summer surface layer above and the stratified ambient water below. We offer a physical explanation of the origin of the observed temperature structure, which is also observed in the inner part of several other West Greenland tidewater glacier fjords with an adjacent ice mélange. Hence, this characteristic temperature structure may be used to delineate the first part of the pathway of subglacial freshwater in this type of fjord.

Data Availability Statement

Processed CTD and xCTD data (https://doi.org/10.1594/PANGAEA.921991) are available at the World Data Center PANGAEA.

Acknowledgments
This study received financial support from Greenland Research Council, Greenland Institute of Natural Resources, Greenland Climate Research Centre, and Canada Excellence Research Chairs program. L. M. was funded by research program VENI with project 016.Veni.192.150 from the Dutch Research Council (NWO). The study forms a contribution to the Arctic Science Partnership (ASP). We appreciate logistic support from the Royal Danish Navy vessel HDMS EJNAR MIKKELSEN and the Greenland Institute of Natural Resources' RV Sanna. We would like to thank Flemming Heinrich, Ivali Lennert, and Air Greenland for field-work assistance.

References

Amundson, J. M., Fahnestock, M., Truffer, M., Brown, J., Lüthi, M. P., & Motyka, R. J. (2010). Ice mélange dynamics and implications for terminus stability, Jakobshavn Isbræ, Greenland. *Journal of Geophysical Research*, *115*, F01005. https://doi.org/10.1029/2009JF001405

Beaird, N. L., Straneo, F., & Jenkins, W. (2018). Export of strongly diluted Greenland meltwater from a major glacial fjord. *Geophysical Research Letters*, *45*, 4163–4170. https://doi.org/10.1029/2018GL077000

Bendtsen, J., Mortensen, J., Lennert, K., & Rysgaard, S. (2015). Heat sources for glacial ice melt in a West Greenland tidewater outlet glacier fjord: The role of subglacial freshwater discharge. *Geophysical Research Letters*, *42*, 4089–4095. https://doi.org/10.1002/2015GL063846

Bendtsen, J., Mortensen, J., & Rysgaard, S. (2015). Modelling subglacial discharge and its influence on ocean heat transport in arctic fjords. *Ocean Dynamics*, *65*(11), 1535–1546. https://doi.org/10.1007/s10236-015-0883-1

Cape, M. R., Straneo, F., Beaird, N., Bundy, R. M., & Charette, M. A. (2019). Nutrient release to oceans from buoyancy-driven upwelling at Greenland tidewater glaciers. *Nature Geoscience*, *12*(1), 34–39. https://doi.org/10.1038/s41561-018-0268-4

Carroll, D., Sutherland, D. A., Shroyer, E. L., Nash, J. D., Catania, G. A., & Stearns, L. A. (2015). Modeling turbulent subglacial meltwater plumes: Implications for fjord-scale buoyancy-driven circulation. *Journal of Physical Oceanography*, *45*(8), 2169–2185. https://doi.org/10.1175/JPO-D-15-0033.1

Chauché, N., Hubbard, A., Gascard, J.-C., Box, J. E., Bates, R., Koppes, M., et al. (2014). Ice-ocean interaction and calving front morphology at two West Greenland tidewater outlet glaciers. *The Cryosphere*, *8*(4), 1457–1468. https://doi.org/10.5194/tc-8-1457-2014

Dukhovskoy, D. S., Yashayaev, I., Proshutinsky, A., Bamber, J. L., Bashmachnikov, I. L., Chassignet, E. P., et al. (2019). Role of Greenland freshwater anomaly in the recent freshening of the subpolar North Atlantic. *Journal of Geophysical Research: Oceans*, *124*, 3333–3360. https://doi.org/10.1029/2018JC014686

Fichefet, T., Poncin, C., Goosse, H., Huybrechts, P., Janssens, I., & LeTreut, H. (2003). Implications of changes in freshwater flux from the Greenland ice sheet for the climate of the 21st century. *Geophysical Research Letters*, *30*(17), 1911. https://doi.org/10.1029/2003GL017826

Gade, H. G. (1979). Melting of ice in sea water: A primitive model with application to the Antarctic ice shelf and icebergs. *Journal of Physical Oceanography*, *9*(1), 189–198. https://doi.org/10.1175/1520-0485(1979)009<0189:MOIISW>2.0.CO;2

Hanna, E., Navarro, F. J., Pattyn, F., Domingues, C. M., Fettweis, X., Ivins, E. R., et al. (2013). Ice-sheet mass balance and climate change. *Nature*, *498*(7452), 51–59. https://doi.org/10.1038/nature12238

Hopwood, M. J., Carroll, D., Browning, T. J., Meire, L., Mortensen, J., Krisch, S., & Achterberg, E. P. (2018). Non-linear response of summertime marine productivity to increased meltwater discharge around Greenland. *Nature Communications*, *9*(1), 3256. https://doi.org/10.1038/s41467-018-05488-8

Jackson, R. H., Nash, J. D., Kienholz, C., Sutherland, D. A., Amundson, J. M., Motyka, R. J., et al. (2020). Meltwater intrusions reveal mechanisms for rapid submarine melt at a tidewater glacier. *Geophysical Research Letters*, *47*, e2019GL085335. http://doi.org/10.1029/2019GL085335

Jackson, R. H., Shroyer, E. L., Nash, J. D., Sutherland, D. A., Carroll, D., Fried, M. J., et al. (2017). Near-glacier surveying of a subglacial discharge plume: Implications for plume parameterizations. *Geophysical Research Letters*, *44*, 6886–6894. https://doi.org/10.1002/2017GL073602

Jenkins, A. (2011). Convection-driven melting near the grounding lines of ice shelves and tidewater glaciers. *Journal of Physical Oceanography*, *41*(12), 2279–2294. https://doi.org/10.1175/JPO-D-11-03.1

Kjeldsen, K. K., Mortensen, J., Bendtsen, J., Petersen, D., Lennert, K., & Rysgaard, S. (2014). Ice-dammed lake drainage cools and raises surface salinities in a tidewater outlet glacier fjord, West Greenland. *Journal of Geophysical Research: Earth Surface*, *119*, 1310–1321. https://doi.org/10.1002/2013JF003034

Kwiatkowski, L., Naar, J., Bopp, L., Aumont, O., Defrance, D., & Couespel, D. (2019). Decline in Atlantic primary production accelerated by Greenland ice sheet melt. *Geophysical Research Letters*, *46*, 11,347–11,357. https://doi.org/10.1029/2019GL085267

Langen, P. L., Rodehacke, C. B., Mottram, R. H., Christensen, J. H., Boberg, F., Stendel, M., et al. (2015). Quantifying energy and mass fluxes controlling Godthåbsfjord freshwater input in a 5 km simulation (1991-2012). *Journal of Climate*, *28*(9), 3694–3713. https://doi.org/10.1175/JCLI-D-14-00271.1

Mankoff, K. D., Ahlstrøm, A. P., Colgan, W., Fausto, R. S., Fettweis, X., Kondo, K., et al. (2020). Greenland liquid water runoff from 1979 through 2017. Earth System Science Data Discussion. https://doi.org/10.5194/essd-2020-47, in review.

Mankoff, K. D., Straneo, F., Cenedese, C., Das, S. B., Richards, C. G., & Singh, H. (2016). Structure and dynamics of a subglacial discharge plume in a Greenlandic fjord. *Journal of Geophysical Research: Oceans*, *121*, 8670–8688. https://doi.org/10.1002/2016JC011764

Meire, L., Mortensen, J., Meire, P., Juul-Pedersen, T., Sejr, M. K., Rysgaard, S., et al. (2017). Marine-terminating glaciers sustain high productivity in Greenland fjords. *Global Change Biology*, *23*(12), 5344–5357. https://doi.org/10.1111/gcb.13801

Mortensen, J., Bendtsen, J., Lennert, K., & Rysgaard, S. (2014). Seasonal variability of the circulation system in a West Greenland tidewater outlet glacier fjord, Godthåbsfjord (64°N). *Journal of Geophysical Research: Earth Surface*, *119*, 2591–2603. https://doi.org/10.1002/2014JF003267

Mortensen, J., Bendtsen, J., Motyka, R. J., Lennert, K., Truffer, M., Fahnestock, M., & Rysgaard, S. (2013). On the seasonal freshwater stratification in the proximity of fast-flowing tidewater outlet glaciers in a sub-Arctic sill fjord. *Journal of Geophysical Research: Oceans*, *118*, 1382–1395. https://doi.org/10.1002/jgrc.20134

Mortensen, J., Lennert, K., Bendtsen, J., & Rysgaard, S. (2011). Heat sources for glacial melt in a subarctic fjord (Godthåbsfjord) in contact with the Greenland ice sheet. *Journal of Geophysical Research*, *116*, C01013. https://doi.org/10.1029/2010JC006528

Mortensen, J., Rysgaard, S., Arendt, K. E., Juul-Pedersen, T., Søgaard, D. H., Bendtsen, J., & Meire, L. (2018). Local coastal water masses control heat levels in a West Greenland tidewater outlet glacier fjord. *Journal of Geophysical Research: Oceans*, *123*, 8068–8083. https://doi.org/10.1029/2018JC014549

Motyka, R. J., Cassotto, R., Truffer, M., Kjeldsen, K. K., van As, D., Korsgaard, N. J., et al. (2017). Asynchronous behavior of outlet glaciers feeding Godthåbsfjord (Nuup Kangerlua) and the triggering of Narsap Sermia's retreat in SW Greenland. *Journal of Glaciology*, *63*(238), 288–308. https://doi.org/10.1017/jog.2016.138

Motyka, R. J., Hunter, L., Echelmeyer, K. A., & Connor, C. (2003). Submarine melting at the terminus of a temperate tidewater glacier, LeConte glacier, Alaska, USA. *Annals of Glaciology*, *36*, 57–65. https://doi.org/10.3189/172756403781816374

Rahmstorf, S. (1995). Bifurcations of the Atlantic thermohaline circulation in response to changes in the hydrological cycle. *Nature*, *378*(6553), 145–149. https://doi.org/10.1038/378145a0

Rietbroek, R., Brunnabend, S.-E., Kusche, J., Schröter, J., & Dahle, C. (2016). Revisiting the contemporary sea-level budget on global and regional scales. *Proceedings of the National Academy of Sciences*, *113*(6), 1504–1509. https://doi.org/10.1073/pnas.1519132113

Rignot, E., & Mouginot, J. (2012). Ice flow in Greenland for the international polar year 2008–2009. *Geophysical Research Letters*, *39*, L11501. https://doi.org/10.1029/2012GL051634

Rysgaard, S., Boone, W., Carlson, D., Sejr, M. K., Bendtsen, J., Juul-Pedersen, T., et al. (2020). An updated view on water masses on the pan-West Greenland continental shelf and their link to proglacial fjords. *Journal of Geophysical Research*, *125*, e2019JC015564. https://doi.org/10.1029/2019JC015564

Rysgaard, S., Mortensen, J., Juul-Pedersen, T., Sørensen, L. L., Lennert, K., Søgaard, D. H., et al. (2012). High air-sea CO_2 uptake rates in nearshore and shelf areas of southern Greenland: Temporal and spatial variability. *Marine Chemistry*, *128-129*, 26–33. https://doi.org/10.1016/j.marchem.2011.11.002

Seifert, M., Hoppema, M., Burau, C., Elmer, C., Friedrichs, A., Geuer, J. K., et al. (2019). Influence of glacial meltwater on summer biogeochemical cycles in Scoresby Sund, East Greenland. *Frontiers in Marine Science*, *6*, 412. https://doi.org/10.3389/fmars.2019.00412

Slater, D. A., Nienow, P., Sole, A., Cowton, T. O. M., Mottram, R., Langen, P., & Mair, D. (2017). Spatially distributed runoff at the grounding line of a large Greenlandic tidewater glacier inferred from plume modelling. *Journal of Glaciology*, *63*(238), 309–323. https://doi.org/10.1017/jog.2016.139

Slater, D. A., Nienow, P. W., Cowton, T. R., Goldberg, D. N., & Sole, A. J. (2015). Effect of near-terminus subglacial hydrology on tidewater glacier submarine melt rates. *Geophysical Research Letters*, *42*, 2861–2868. https://doi.org/10.1002/2014GL062494

Stevens, L. A., Straneo, F., Das, S. B., Plueddemann, A. J., Kukulya, A. L., & Morlighem, M. (2016). Linking glacially modified waters to catchment-scale subglacial discharge using autonomous underwater vehicle observations. *The Cryosphere*, *10*(1), 417–432. https://doi.org/10.5194/tc-10-417-2016

Stouffer, R. J., Yin, J., Gregory, J. M., Dixon, K. W., Spelman, M. J., Hurlin, W., et al. (2006). Investigating the causes of the response of the thermohaline circulation to past and future climate changes. *Journal of Climate*, *19*(8), 1365–1387. https://doi.org/10.1175/JCLI3689.1

Straneo, F., Curry, R. G., Sutherland, D. A., Hamilton, G. S., Cenedese, C., Våge, K., & Stearns, L. A. (2011). Impact of fjord dynamics and glacial runoff on the circulation near Helheim glacier. *Nature Geoscience*, *4*(5), 322–327. https://doi.org/10.1038/NGEO1109

Thornalley, D. J. R., Oppo, D. W., Ortega, P., Robson, J. I., Brierley, C. M., Davis, R., et al. (2018). Anomalously weak Labrador Sea convection and Atlantic overturning during the past 150 years. *Nature*, *556*(7700), 227–230. https://doi.org/10.1038/s41586-018-0007-4

Washam, P., Nicholls, K. W., Münchow, A., & Padman, L. (2019). Summer surface melt thins Petermann Gletscher ice shelf by enhancing channelized basal melt. *Journal of Glaciology*, *65*(252), 662–674. https://doi.org/10.1017/jog.2019.43

Wu, P., Wood, R., & Stott, P. (2004). Does the recent freshening trend in the North Atlantic indicate a weakening thermohaline circulation? *Geophysical Research Letters*, *31*, L02301. https://doi.org/10.1029/2003GL018584

Yang, Q., Dixon, T. H., Myers, P. G., Bonin, J., Chambers, D., van den Broeke, M. R., et al. (2016). Recent increases in Arctic freshwater flux affects Labrador Sea convection and Atlantic overturning circulation. *Nature Communications*, *7*(1), 10,525. https://doi.org/10.1038/ncomms10525